Load shifting versus manual frequency reserve: Which one is more appealing to flexible loads?

Peter A.V. Gade*†, Trygve Skjøtskift†, Henrik W. Bindner*, Jalal Kazempour*
*Department of Wind and Energy Systems, Technical University of Denmark, Kgs. Lyngby, Denmark
†IBM Client Innovation Center, Copenhagen, Denmark

***Abstract*— This paper investigates how a flexible load can deliver flexibility for manual frequency reserves and load shifting. We discuss the advantages and disadvantages of the two and their appeal from a monetary point of view. To this end, a grey-box model of a supermarket freezer is created to describe its temperature dynamics using real data from a supermarket in Denmark. A two-stage stochastic mixed-integer linear program (MILP) maximizes the flexibility value from the freezer where two solution strategies for manual frequency reserves are presented. Load shifting shows to be more profitable than manual frequency reserves on unseen price data, but is also more consequential for the temperature in the freezer than flexibility provision for manual frequency reserves.**

***Index Terms*—Demand-side flexibility.**

I. Introduction

Power consumers are looking to reduce costs by any means due to sky-rocketing power- and gas prices. In Denmark, supermarkets are especially exposed due to their high energy consumption, and they are actively looking into initiatives to reduce their electricity bill. One of these initiatives is demand-side flexibility, whereby a supermarket can shift consumption in time when spot prices are lower or when the power grid needs up-regulation. There are thousands of supermarkets in Denmark, willing to provide flexibility, and their thermostatically controlled loads (TCLs) are especially suited for this. However, the monetary benefit still remains uncertain. In this paper, we describe how to estimate and utilize a supermarket freezer's flexibility with respect to manual frequency reserves and load shifting.

There are also a lot of initiatives in Denmark to harness demand-side flexibility. For example, IBM is currently developing a software platform - called Flex Platform - that can harness flexibility from industrial and commercial consumers for bidding in ancillary service markets by a balance responsible party (BRP). One large supermarket chain in Denmark has already signed up for the Flex Platform, and another supermarket chain is currently exploring the possibility of joining. In order to understand the flexibility of freezers, one must first understand the working of freezers, their temperature dynamics, and how they are controlled.

Corresponding author. Tel.: +45 24263865.
Email addresses: pega@dtu.dk (P.A.V. Gade), Trygve.Skjotskift@ibm.com (T. Skjøtskift), hwbi@dtu.dk (H.W. Bindner), jalal@dtu.dk (J. Kazempour).
Manuscript received April 19, 2021; revised August 16, 2021.

To this end, many studies have used grey-box models to capture the most fundamental physics while using data to calibrate the model. A grey-box model can illustrate the concept of flexibility well, and we show how it can be used for simulations. Such a model can also readily be used in a mathematical optimization framework to, e.g., reduce costs or maximize earnings from flexibility. An optimization model can be used to obtain a simple policy for how to shift consumption in time and how to provide flexibility in the form of manual frequency reserves, also called mFRR[1]. In this work, we determine the monetary benefit of flexibility using such a optimization model with two solution strategies: 1) one using a five days lookback and 2) one using 2021 data. We evaluate the model on unseen 2022 price data.

A. Dilemma: mFRR vs load shifting

Furthermore, for consumers that are actively looking to reduce costs, it is important to understand the monetary benefit of flexibility. From their perspective, it is natural to first look into load shifting at first since it is the most obvious and easy way to utilize flexibility. Here, load shifting simply refers to shifting consumption to a point in time, typically when spot prices are lower.

However, load shifting is not necessarily helping the power grid. In fact, if a significant amount of consumers started to do it, it could be detrimental to the power grid by moving peak consumption to a different time of the day. Intriguingly, many industrial and residential consumers have already started doing that to some degree as a response to the energy crisis. As a result, load shifting might provide *short-term* monetary benefit, but it is not necessarily helping the power grid in the long run.

Instead, consumers could opt for ancillary services for which they are paid for providing flexibility through an *aggregator*. One such service is mFRR in Denmark, which is a slow-responding reserve used to stabilize the frequency in the power grid. mFRR resembles load shifting in the sense that it is the largest energy reserve operated by the transmission system operator (TSO), and can be provided by consumers by shifting their consumption in time.[2]

[1]**mFRR**: manual frequency restoration reserves. The term will be used for the remainder of the paper and is equivalent to tertiary reserves.

[2]Likewise, generators provide mFRR by increasing their power generation.

0000–0000/00$00.00 © 2021 IEEE

The demand response for consumers participating in mFRR versus load shifting will therefore look similar. From the consumers' perspective, it is of great interest to investigate the monetary benefit of participating in each, and it is important to understand the incentive of consumers to participate in mFRR from a TSO perspective as well.

B. Research questions

To understand the incentives to participate in load shifting and mFRR from a flexible consumer's perspective, this work aim to investigate and answer the following research questions:

- How can a supermarket freezer's flexibility be characterized?
- How much monetary benefit can a freezer provide for mFRR?
- How much monetary benefit can a freezer provide for load shifting?
- What are the advantages and disadvantages of participating in mFRR versus load shifting?

Some of these questions have been looked at extensively in literature, so we first provide a brief literature review to pinpoint where new work is required and how our work relates to existing work.

C. Literature review and our contributions

Demand-side flexibility has been extensively studied. The approach taken in each study is very much dependent on whose perspective from which the flexibility is utilized. Often, full knowledge and control is assumed. An often overlooked, implicit assumption is that the aggregator and/or trading entity are the same with an exclusive business relationship to flexible consumer [1]. The incentives and investments required for delivering flexibility for the flexible consumer are often overlooked as well. Many also assume an idealized market mechanism or simply propose a new mechanism for trading flexibility while we look at the status quo today.

In [2], a complete white-box model of a supermarket refrigeration system is presented and validated against real-life data. It is also shown how such a system can provide a demand-response. This work serves as a good benchmark for any grey-box model of a supermarket refrigeration system. However, such an approach is hard to scale and requires complete knowledge of every refrigeration system. A very similar approach is taken in [3] and [4]. In [5], a second-order model is used to model the food and air temperature in a freezer in an experimental setting. It is shown how the food temperature has much slower dynamics than the air temperature. In [6], a simple first-order virtual battery model for a TCL is presented. This model also constitutes the starting point for modelling temperature dynamics in this report as it has a powerful, physical interpretation. A similar *bucket* model is introduced in [7].

In [8], the grey-box modelling approach to a refrigeration system is described in detail from formulation to validation. They use the grey-box model for model predictive control (MPC) for load shifting. In [9], an ARMAX time-series model is used to characterize the temperature development of supermarket freezers and refrigerators. It is validated on one-step prediction errors, and the authors also note how it is able to roughly simulate the system over a longer period as well. This classical time-series approach provides an alternative to the state-space approach. The authors show how MPC with three different objectives can be used to optimize the flexibility in the system using the ARMAX model.

In [10], a MILP formulation is used to specifically address up- and down-regulation hours from a baseline consumption. It is assumed that the energy for down-regulation is equal to the energy not consumed when up-regulating. A similar approach is taken in our work except we will define use down-regulation until the temperature state is (approximately) back to its setpoint.

In [11], [12], [13], and [13], residential air condition units are modelled using up- and down-regulation blocks characterizing the flexibility. The blocks are obtained from grey-box models of households [14]. The authors show how such a block formulation can be solved using exact and stochastic dynamic programming in the context of peak shaving demand for a utility in the US. The demand-side flexibility then functions as a hedge towards extreme electricity prices. Although such a use case has not been relevant in Denmark yet, the estimation of flexibility blocks is a novel idea as it avoids having to explicitly integrate a physical model into an optimization problem. However, the tradeoff is that the curse of dimensionality quickly makes dynamic programming computationally intractable for a large portfolio of heterogenous demand-side assets. Furthermore, it might be difficult to assure the Markov property [15] when reformulating the problem even slightly.

Flexibility blocks are also used in [16] for an offering strategy. Here, the flexibility blocks were derived from measurements of residential appliances in the Ecogrid 2.0 project [17].

In [18] and [19], the authors describe how flexibility interfaced with pre-defined flexibility characteristics allow aggregators to utilize and contract the flexibility. This assumes flexibility of the demand-side assets is fully known beforehand. However, this type of information flexibility interface and flexibility contract specification is still useful for aggregators when engaging with consumers with well-known assets at the point where aggregation of demand-side flexibility is a mature and prevalent business.

In [20] a portfolio of residential heat pumps are modelled using a linear, first-order model. Individual heat pumps are lumped together as essentially one big, aggregated heat pump as described in [21]. The first-order model is a grey-box model incorporating the physics, i.e., the temperature dynamics in household. Such an approach will be used in this work as well. The authors also consider how the portfolio of heat pumps can be used for spot price optimization and real-time bidding in the balancing market but do not consider mFRR. However, they assume that all the assets can be controlled continuously in an economic model predictive control (E-MPC) setting. The temperature deviations are minimized directly in the objective function using the integrated error

of total temperature deviations. This introduces a trade-off parameter in the objective function that must be tuned to weigh economic value versus temperature deviation to the setpoint. A close, integrated relationship between the BRP, aggregator, and consumer is assumed.

To the best of our knowledge, there is no work that investigated the monetary incentives for providing mFRR versus load shifting, respectively, although both have been studied extensively. This work aims to fill that gap. Furthermore, when stating the objective functions for mFRR, most studies have assumed a simplified market structure, and neglect the fact that the aggregator and the consumer are not necessarily the same entity. We discuss the consequences of this assumption in relation to the market structure in Denmark [1], and in the context of mFRR and load shifting.

D. Outline

The rest of the paper is organized as follows. In Section II, modelling of TCLs using grey-box models is described using real data of a supermarket freezer in Denmark. Thereafter, mFRR and load shifting are described in detail and their objective functions are stated. In Section III, the optimization problem is presented, both in compact and final form. Furthermore, two solution strategies for solving the optimization problem for mFRR are introduced. In Section IV, the results of the case study are presented and discussed. Finally, Section V concludes the paper.

II. Monetizing flexibility from TCLs

There are several ways to monetize flexibility from TCLs. In this section, we focus on mFRR and load shifting. First, we describe how to mathematically model a TCL as a flexible resource. Second, we describe how to monetize the flexibility from TCLs for mFRR and load shifting and provide the objective functions in both cases. For mFRR, the objective function include all costs and revenues for the BRP, while for load shifting, the objective function only includes the flexible demand's perspective. This approach explicitly shows the situation where flexible demand take actions without including the BRP as this is more realistic.

A. Modelling TCL as a flexible resource

TCLs are characterized by being controlled such that the temperature is kept at a specified setpoint. Examples includes heat pumps, freezers, air condition units, ovens, etc. They are widely believed to constitute an important part of demand-side flexibility due to the inherent thermal inertia of such temperature-driven systems.

In this paper, we focus on freezers, which are a very common type of TCLs. Specifically, we focus on a single freezer display in a Danish supermarket. Freezers are characterized by a large thermal inertia due to the frozen food, which makes them suitable for flexibility. On the other hand, there is a risk of food degradation when utilizing flexibility. Therefore, it is important to model the temperature dynamics in the freezer for a realistic and risk-aware estimation of its flexibility.

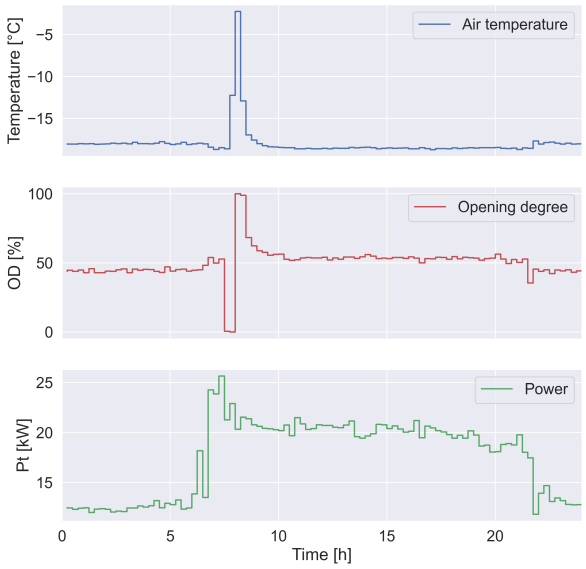

Fig. 1. **Top**: average temperature of a single freezer in a supermarket. **Middle**: average opening degree of the freezer expansion valve. **Bottom**: average power of the compressors feeding all the freezers (scaled to only include all freezers in the supermarket).

The rest of the section is organized as follows. First, we visualize the measurements from a real supermarket freezer. Second, we introduce a second-order grey-box model that characterizes the supermarket freezer. Third, we validate the second-order model and show how it can be used to simulate a demand response from a freezer.

1) Supermarket freezer: In this paper, data from a large Danish supermarket for a single freezer is used as a case study. In Figure 1, the temperature, opening degree, and power of the freezer is shown as an average for all hours in a day over a year. The temperature fluctuates around its setpoint at -18 °C with the exception of hour 7-8 where defrosting is scheduled. While defrosting, a heating element is turned on briefly, and the expansion valve is closed such that the flow of refrigerant stops. Afterwards, while recovering the temperature, the expansion valve is opened fully again. The power consumption of the whole compressor rack is shown in the bottom plot. The power consumption is highest during opening hours, and it is lowest during closing hours. During opening hours, food is being replaced and customers open the display case constantly. Furthermore, most supermarkets puts additional insulation on the display cases during closing hours which reduced thermal losses. For these reasons, there are effectively two regimes for a supermarket freezer plus a short defrosting regime.

2) Thermal modelling of freezer: In [6], it is described how a simple TCL model can be made. We extend it to a second-order model that accounts for the thermal mass of the food, which essentially provides the flexibility in freezers:

TABLE I
PARAMETER ESTIMATES OF (2).

Parameter	Value	Unit
C^f	5.50	kWh/°C
C^c	0.13	kWh/°C
R^{cf}	4.91	°C/kW
$R^{ci,day}$	25.6	°C/kW
$R^{ci,night}$	46.5	°C/kW
η	2.38	
ϵ	6.477	°C/h

$$\frac{dT^f(t)}{dt} = \frac{1}{C^f}\left(\frac{1}{R^{cf}}(T^c(t) - T^f(t))\right) \tag{1a}$$

$$\frac{dT^c(t)}{dt} = \frac{1}{C^c}\Big(\frac{1}{R^{cf}}(T^f(t) - T^c(t)) + \frac{1}{R^{ci}(t)}(T^i(t) - T^c(t)) - \frac{1}{n}\eta \cdot OD(t)P(t)\Big) + \epsilon \mathbb{1}^{df} \tag{1b}$$

In state-space form, the system in (1) is:

$$T^f_{t+1} = T^f_t + dt \cdot \frac{1}{C^f}\left(\frac{1}{R^{cf}}(T^c_t - T^f_t)\right) \tag{2a}$$

$$T^c_{t+1} = T^c_t + dt \cdot \frac{1}{C^c}\Big(\frac{1}{R^{cf}}(T^f_t - T^c_t) + \frac{1}{R^{ci}_t}(T^i_t - T^c_t) - \frac{1}{n}\eta \cdot OD_t P_t\Big) + \epsilon \mathbb{1}^{df} \tag{2b}$$

Here, T^c is the air temperature in the freezer, and T^f is the food temperature which is a latent, unobserved state. It is essentially a low-pass filter of the air temperature in the freezer with time constant $\tau = C^f R^{cf}$. C^f and C^c are the thermal capacitance of the food and air in the freezer, respectively. R^{cf} and R^{ci} are the thermal resistance between food and air in the freezer, and air and indoor temperature, respectively. Furthermore, ϵ represents the temperature change when defrosting and $\mathbb{1}^{df}$ is an indicator for when defrosting happens. R^{ci} is time-varying to capture the differences between opening- and closing hours. The opening degree, OD_t, and power P_t, are exogenous inputs. In this work, only P_t is controllable. n is the number of freezers in the supermarket, and η is the compressor efficiency. The model is discretized with a time step of 15 minutes, i.e. $dt = 0.25$ hours.

3) Model validation: Using the R library CTSM-R [22], the parameters in (2) have been estimated as shown in Table I. Notice that the thermal capacitance of the air in the freezer is significantly smaller than the thermal capacitance of the food, indicating that that the food temperature changes comparatively slower. The thermal resistance between the food and air inside the freezer, R^{cf}, is also significantly smaller than the thermal resistance between the air in the freezer and the indoor temperature in the supermarket, R^{ci}, both during the day and the night. This makes sense as the lid acts as a physical barrier insulating the freezer. Furthermore, the thermal resistance to the indoor air temperature is higher during the night which means that less power is needed as seen in Figure 1.

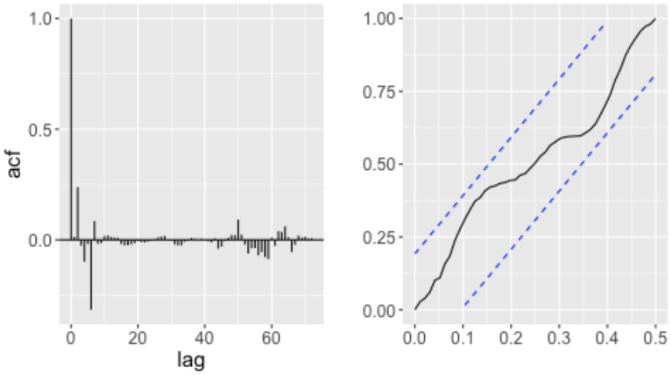

Fig. 2. Validation of the state-space model in (2). **Left**: auto-correlation function of the model residuals. **Right**: cumulated periodogram of the residuals.

The model residuals calculated from the one-step ahead prediction errors should ideally resemble white noise in order for a model to capture all dynamics [23]. Figure 2 shows the auto-correlation and cumulated periodogram of the residuals. The autocorrelation shows two significant lags for lag two and seven, but looks good otherwise. Likewise, in the periodogram, it seems the model is able to capture most dynamics at all frequencies.

Furthermore, Figure 3 (left) shows a 24-hour simulation of (2). It is seen that the simulation is very reasonable and closely follows the measured air temperature. However, it is quite difficult to capture the dynamics when, and immediately after, defrosting. Nevertheless, the model residuals appears to resemble white noise otherwise, and the simulation is accurate as well. It is therefore deemed that the model is good enough to proceed.

In Figure 3 (right), an example of a demand response event is shown. It can clearly be seen how the air temperature increases when the power is turned off, and how it decreases when the power is turned back on. The food temperature is much more stable and only changes slightly, as expected. The rebound occurs until the food temperature is back to its normal value.

B. mFRR

mFRR is a slow-responding reserve which is activated after primary and secondary reserves in order to restore the frequency in the power grid to 50 Hz. The market for mFRR is usually operated by each country's respective TSO.[3]

Figure 4 shows the timeline of the mFRR market in Denmark.[4] First, BRPs can bid reserve capacities in each hour, $p^{r,\uparrow}_h \ \forall h \in \{1, \dots 24\}$, in the market for the next day, D. If accepted, they receive the reservation price, $\lambda^{r,\uparrow}_h$. This happens *before* the day-ahead market clearing for which the BRPs buy energy for their expected demand, P^{Base}_h, at the spot price, λ^s_h. After that, a regulating power bid, λ^{bid}_h, must be submitted for each hour in D where $p^{r,\uparrow}_h > 0$. In real-time, the reserves are activated if the following conditions hold, depending on the balancing price, λ^b_h:

[3]In Denmark, the TSO is Energinet.
[4]There is only a market for up-regulation.

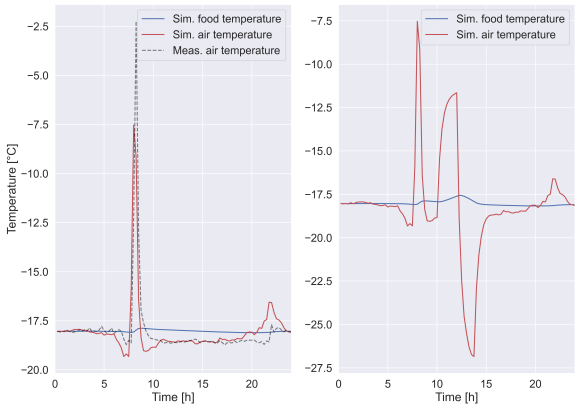

Fig. 3. **Left**: Simulation of (2) using the parameters in Table I. **Right**: Simulation where power is turned off for two hours with a subsequent rebound at the nominal power until the food temperature is back to its normal value.

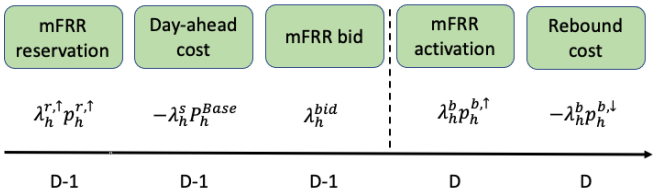

Fig. 4. Timeline of the Danish mFRR market.

- $p_h^{r,\uparrow} > 0$
- $\lambda_h^{\text{bid}} < \lambda_h^b$
- $\lambda_h^b > \lambda_h^s$

If the conditions are met, the BRP receives the balancing price times their actual up-regulation, $p_h^{b,\uparrow}$. The BRP also incurs an additional cost due to any subsequent rebound. Furthermore, the BRP incurs a penalty, $s_h = \max\{0, p_h^{r,\uparrow} - p_h^{b,\uparrow}\}$, if they don't deliver their promised reserve.

A suitable objective function for a BRP delivering mFRR up-regulation for one day is therefore:

$$\text{Objective mFRR} = \underbrace{-\sum_{h=1}^{24} \lambda_h^s P_h^{\text{Base}}}_{\text{Energy cost}} + \underbrace{\sum_{h=1}^{24} \lambda_h^r p_h^{r,\uparrow}}_{\text{Reservation payment}} + \underbrace{\sum_{h=1}^{24} \lambda_h^b p_h^{b,\uparrow}}_{\text{Activation payment}} \underbrace{- \sum_{h=1}^{24} \lambda_h^b p_h^{b,\downarrow}}_{\text{Rebound cost}} \underbrace{- \sum_{h=1}^{24} \lambda^p s_h}_{\text{Penalty cost}} \tag{3}$$

C. Load shifting

Another option for utilizing flexibility is to shift the load to a different time according to the spot prices which are known already 12-36 hours in advance. Then it is simply a matter of consuming in low-price hours and not in high-price hours.

For a TCL, there are additional constraints to how the energy can be shifted and for the rebound. First, there can be temperature constraints which will result in less energy being shifted. Second, the rebound must happen immediately before or after reducing power consumption (otherwise, the temperature deviation becomes too big).

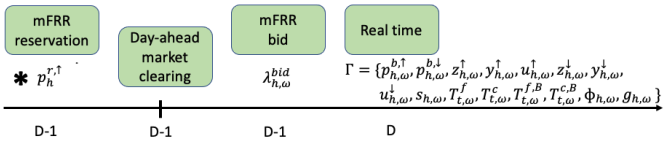

Fig. 5. Variables related to mFRR up-regulation decisions. The asterisk indicates the first-stage decision.

The savings from load shifting are directly proportional to the volume and price difference between the shifted load and baseline load as given by:

$$\text{Load shifting savings} = \sum_{h=1}^{24} \lambda_h^s p_h^{\text{Base}} - \lambda_h^s p_h' \tag{4}$$

where p_h' is the flexible power profile, p_h^{Base} is the baseline power, and λ_h^s is the spot price.

However, since the load shifting action only occurs *after* the day-ahead market clearing (cf. Figure 4), the BRP has already bought $\lambda_h^s p_h^{\text{Base}}$ and any deviation results in an imbalance for the BRP. In this work, we look at the case where the flexible demand acts selfishly and excludes the BRP from its load shifting action. Therefore, the objective function for the flexible demand is simply:

$$\text{Objective load shifting} = \sum_{h=1}^{24} \lambda_h^s p_h' \tag{5}$$

III. Optimization Model and Solution Strategy

In this section, the optimization problem is presented. First, the time sequence of decision variables for mFRR is presented. Second, we explain how scenarios for price data are generated for in-sample (IS) training and out-of-sample (OOS) evaluation. Third, we present the compact model formulation. Fourth, we present the two solution strategies for mFRR, including the mFRR bidding policy and scenario decomposition. Finally, we present the full model formulation.

A. Time sequence for decision making

Figure 5 shows the stages for making decisions in the mFRR market. First, a reservation bid, $p_h^{r,\uparrow}$ is submitted. For any reservation bid accepted, a regulating power bid must be submitted, $\lambda_{h,\omega}^{\text{bid}}$. The reservation and bid are the *first-stage* decisions. The set Γ_ω, contains all real-time variables in the optimization problem and are the *second-stage* decisions. They control the real-time power, auxillary variables for identifying up- and down-regulation[5], temperature dynamics, and when to deliver up-regulation according to the bid. For more details, see Section III-E. The index, ω, specifies a scenario.

[5]Down-regulation refers to the rebound action in this context.

B. Scenario generation

To train the optimization model to get a policy for $p_h^{r,\uparrow}$ and $\lambda_{h,\omega}^{\text{bid}}$, we generate scenarios for price data using two strategies (where one scenario corresponds to one day):

1) Training IS on 2021 price data with varying number of scenarios
2) Training IS using a lookback of five days

In both cases, balancing prices, λ_h^b, are sampled from days where up-regulation happened $1 \ldots 24$ hours with equal probability. In this way, there is emphasis on days and hours where up-regulation happened, and the model should learn a policy taking this into account.

For spot prices, the lookback strategy uses the spot price from the past five days to take advantage of any autocorrelation. The first strategy samples spot price days in 2021. For both strategies, evaluation is done OOS on unseen 2022 price data.

For load shifting, the policy is simply to solve the optimization problem for the next day since the day-ahead market clearing happens in advance.

C. Compact model formulation

The compact model formulation is presented in Problem 6. The objective function is the sum of the revenue from the reservation bid, i.e., first-stage decisions, and the *expected* revenue and costs from the regulating power bid and subsequent rebound and penalties. Constraint (6b) incorporates activation of the bid, and constraint (6c) incorporates the temperature dynamics in the freezer.

$$\max_{\boldsymbol{p}^{r,\uparrow},\boldsymbol{\lambda}_{\omega}^{\text{bid}},\boldsymbol{\Gamma}_{\omega}} \quad f(\boldsymbol{p}^{r,\uparrow}) + \sum_{\omega} \pi_{\omega} g(\boldsymbol{\Gamma}_{\omega}) \tag{6a}$$

$$s.t \quad h(\boldsymbol{p}^{r,\uparrow}, \boldsymbol{\lambda}_{omega}^{\text{bid}}, \boldsymbol{\Gamma}_{\omega}) \leq 0, \quad \forall \omega \tag{6b}$$

$$\text{State-space model in } (2), \quad \forall \omega \tag{6c}$$

$$\Big(\boldsymbol{p}^{r,\uparrow}, \boldsymbol{\lambda}_{\omega}^{\text{bid}}, \boldsymbol{p}_{\omega}^{b,\uparrow}, \boldsymbol{p}_{\omega}^{b,\downarrow}, \boldsymbol{s}_{\omega}, \boldsymbol{T}_{\omega}^{c}, \boldsymbol{T}_{\omega}^{f}, \boldsymbol{T}_{\omega}^{c,B}, \boldsymbol{T}_{\omega}^{f,B}, \boldsymbol{\phi}_{\omega}, \boldsymbol{g}_{\omega}\Big) \in \mathbb{R}^n \tag{6d}$$

$$\boldsymbol{u}_{\omega}, \boldsymbol{z}_{\omega}, \boldsymbol{y}_{\omega} \in \{0,1\} \tag{6e}$$

For mFRR, the objective function in (3) corresponds to f and g in (6a). For load shifting, the optimization problem is simply obtained by removing bid constraints and replacing the (6a) with (5), and then solving the optimization problem for the next day.

D. Solution strategy

To solve Problem (6), we first need to specify a bidding policy that can readily be used OOS. We do so by choosing an affine bidding policy. It is then shown how the bidding policy is implemented using McCormick relaxation. Finally, it shown how to solve (6) for many scenarios using decomposition.

1) Affine bidding policy: A bidding policy needs to be easy to follow OOS for the trader. We choose an affine bidding policy, i.e., a linear function of the spot price. The bidding policy is given by:

$$\lambda_{h,\omega}^{bid} = \alpha \lambda_{h,\omega}^{s,\text{diff}} + \beta + \lambda_{h,\omega}^{s}, \quad \forall \omega, \forall h \in \{1 \ldots 23\} \tag{7a}$$

$$\alpha \geq 0 \tag{7b}$$

$$\beta \geq 0 \tag{7c}$$

Here, the idea in (7) is that the spot price differential approximates a reasonable policy since a large price differential in hour h means that the spot price at time $h+1$ is much higher. Hence, a large bid at time h is desirable such that the probability of being activated in hour h and rebounding in an expensive hour $h+1$ is low (cf. Section II-B).

Variables α and β is then learned IS and fixed for OOS evaluation. After the day-ahead market clearing, (7) can easily be used to specify bids for the next day, i.e., $\lambda_{h,\omega}^{\text{bid}}$.

2) McCormick relaxation: As explained in Section II-B, activation of mFRR reservation only happens when certain price conditions are met. This is formalized in the following constraint:

$$p_{h,\omega}^{b,\uparrow} + s_{h,\omega} \geq p_h^{r,\uparrow} \cdot \mathbb{1}_{h,\omega}^{(\lambda_h^{bid} < \lambda_{h,\omega}^{b}, \lambda_{h,\omega}^{b} > \lambda_h^{s})}, \quad \forall h, \omega \tag{8}$$

Eq. (8) says that the real-time up-regulation plus a slack variable must be greater than or equal to the reservation if the bid is lower than the balancing price and if up-regulation is needed in hour h. It is a bi-linear constraint so McCormick relaxation is used to convert (8) to a linear constraint by introducing auxillary variables, $\phi_{h,\omega}$ and $g_{h,\omega}$:

$$\lambda_{h,\omega}^{b} - \lambda_h^{s} \geq \lambda_{h,\omega}^{bid} - M \cdot (1 - g_{h,\omega}), \quad \forall h, \omega \tag{9a}$$

$$\lambda_{h,\omega}^{bid} \geq \lambda_{h,\omega}^{b} - \lambda_h^{s} - M \cdot (1 - g_{h,\omega}), \quad \forall h, \omega \tag{9b}$$

$$p_{h,\omega}^{b,\uparrow} \leq \phi_{h,\omega} \cdot \mathbb{1}_{h,\omega}^{\lambda_{h,\omega}^{b} > \lambda_h^{s}}, \quad \forall h, \omega \tag{9c}$$

$$p_{h,\omega}^{b,\uparrow} + s_{h,\omega} \geq \phi_{h,\omega} \cdot \mathbb{1}_{h,\omega}^{\lambda_{h,\omega}^{b} > \lambda_h^{s}}, \quad \forall h, \omega \tag{9d}$$

$$-g_{h,\omega} \cdot M \leq \phi_{h,\omega}, \quad \forall h, \omega \tag{9e}$$

$$\phi_{h,\omega} \leq g_{h,\omega} \cdot M, \quad \forall h, \omega \tag{9f}$$

$$-(1 - g_{h,\omega}) \cdot M \leq \phi_{h,\omega} - p_h^{r,\uparrow}, \quad \forall h, \omega \tag{9g}$$

$$\phi_{h,\omega} - p_h^{r,\uparrow} \leq (1 - g_{h,\omega}) \cdot M, \quad \forall h, \omega \tag{9h}$$

Constraints (9a-9b) ensures that $g_{h,\omega} = 1$ when the balancing price minus the spot price is larger than our bid, λ_h^{bid}, and zero otherwise. Constraints (9c-9d) sets the TCL up-regulation equal to $\phi_{h,\omega}$ (or incurs a penalty) if there is an up-regulation event in the system, i.e., if $\mathbb{1}_{h,\omega}^{\lambda_{h,\omega}^{b} > \lambda_h^{s}} = 1$. Constraints (9e-9f) ensures that $\phi_{h,\omega} = 0$ when $g_{h,\omega} = 0$, i.e., when the balancing price differential is smaller than our bid. Constraints (9g-9h) ensures that $\phi_{h,\omega}$ is equal to the reservation capacity, $p_h^{r,\uparrow}$, whenever $g_{h,\omega} = 1$, i.e., whenever the bid is smaller than the balancing price differential.

3) Scenario decomposition with ADMM: When solving Problem (6) with many scenarios, it quickly becomes computationally intractable due to the number of binaries and intertemporal constraints. To solve it, the Alternating Direction Method of Multipliers (ADMM) algorithm is used which is a decomposition method that solves a large-scale optimization problem by decomposing it into smaller subproblems [24]. In (6), each scenario is solved as a subproblem by setting:

$$\boldsymbol{p}^{r,\uparrow} \rightarrow \boldsymbol{p}^{r,\uparrow}_{\omega}, \quad \alpha \rightarrow \alpha_{\omega}, \quad \beta \rightarrow \beta_{\omega} \tag{10}$$

The ADMM algorithm will converge by achieving consensus on first- and second-stage stage decisions, but it is only a heuristic for MILPs [25].

E. Final model formulation

The final optimization model is a two-stage stochastic MILP and is described in full detail in this subsection. First, all auxillary variables and constraints are presented. Second, constraints related to the power consumption for the freezer is shown. Third, the physical constraints for the temperatures are presented. Lastly, the rebound constraints are presented.

1) Auxillary variables and constraints: First, we describe the necessary auxillary variables and constraints to identify when up- and down-regulation occurs compared to the baseline power, P_h^{Base}. This is required since the costs and revenues from up-regulation and rebound must be determined explicitly. We therefore introduce the following six binary variables [26]:

- $u^{\uparrow}_{h,\omega} \in \{0,1\}$ equal to 1 when starting to deliver up-regulation
- $y^{\uparrow}_{h,\omega} \in \{0,1\}$ equal to 1 during up-regulation
- $z^{\uparrow}_{h,\omega} \in \{0,1\}$ equal to 1 when to stopping up-regulation
- $u^{\downarrow}_{h,\omega} \in \{0,1\}$ equal to 1 when starting to deliver down-regulation
- $y^{\downarrow}_{h,\omega} \in \{0,1\}$ equal to 1 during down-regulation
- $z^{\downarrow}_{h,\omega} \in \{0,1\}$ equal to 1 when to stopping down-regulation

The following constraints implements the logic:

$$u^{\uparrow}_{h-1,\omega} - u^{\uparrow}_{h,\omega} + y^{\uparrow}_{h,\omega} - z^{\uparrow}_{h,\omega} = 0 \quad \forall \omega, \forall h = \{2 \dots 24\} \tag{11a}$$
$$y^{\uparrow}_{h,\omega} + z^{\uparrow}_{h,\omega} \leq 1 \quad \forall h, \omega \tag{11b}$$
$$u^{\downarrow}_{h-1,\omega} - u^{\downarrow}_{h,\omega} + y^{\downarrow}_{h,\omega} - z^{\downarrow}_{h,\omega} = 0 \quad \forall \omega, \forall h = \{2 \dots 24\} \tag{11c}$$
$$y^{\downarrow}_{h,\omega} + z^{\downarrow}_{h,\omega} \leq 1 \quad \forall h, \omega \tag{11d}$$
$$u^{\uparrow}_{h,\omega} + u^{\downarrow}_{h,\omega} \leq 1 \quad \forall h, \omega \tag{11e}$$
$$y^{\uparrow}_{h,\omega} + y^{\downarrow}_{h,\omega} \leq 1 \quad \forall h, \omega \tag{11f}$$
$$z^{\uparrow}_{h,\omega} + z^{\downarrow}_{h,\omega} \leq 1 \quad \forall h, \omega \tag{11g}$$

2) Power constraints: The power consumption of the freezer is constrained by:

$$p_{h,\omega} = P_h^{\text{Base}} - p^{b,\uparrow}_{h,\omega} + p^{b,\downarrow}_{h,\omega}, \quad \forall h, \omega \tag{12a}$$
$$p_h^{r,\uparrow} \leq P_h^{\text{Base}}, \quad \forall h \tag{12b}$$
$$p^{b,\uparrow}_{h,\omega} \leq p_h^{r,\uparrow} \mathbb{1}^{\lambda^b_{h,\omega} > \lambda^s_h}_{h,\omega}, \quad \forall h, \omega \tag{12c}$$
$$p^{b,\uparrow}_{h,\omega} \leq u^{\uparrow}_{h,\omega}(P_h^{\text{Base}} - P^{Min}), \quad \forall h, \omega \tag{12d}$$
$$p^{b,\downarrow}_{h,\omega} \leq u^{\downarrow}_{h,\omega}(P^{\text{Nom}} - P_h^{\text{Base}}), \quad \forall h, \omega \tag{12e}$$
$$P^{Min} \leq p_{h,\omega} \leq P^{\text{Nom}}, \quad \forall h, \omega \tag{12f}$$
$$0 \leq s_{h,\omega} \leq P_h^{\text{Base}}, \quad \forall h, \omega \tag{12g}$$
$$p^{b,\uparrow}_{h,\omega} + s_{h,\omega} \geq p_h^{r,\uparrow} \cdot \mathbb{1}^{(\lambda^{bid}_h < \lambda^b_{h,\omega}, \lambda^b_{h,\omega} > \lambda^s_h)}_{h,\omega}, \quad \forall h, \omega \tag{12h}$$
$$p^{b,\downarrow}_{h,\omega} \geq 0.10 \cdot u^{\downarrow}_{h,\omega}(P^{\text{Nom}} - P_h^{\text{Base}}), \quad \forall h, \omega \tag{12i}$$
$$p_h^{r,\uparrow} \leq P_h^{\text{Base}}(1 - \mathbb{1}^{df}_h), \quad \forall h \tag{12j}$$

Constraint (12a) sets the power equal to the baseline power unless there is up- or down-regulation. Constraint (12b) bounds the reservation power to the baseline power. Constraint (12c) ensures that up-regulation is zero when the system does not need it, and at the same time bounds it to the reservation power. Constraint (12d) ensures that up-regulation is 0 whenever $u^{\uparrow}_{h,\omega} = 0$, and otherwise bounded to the maximum power that can be upregulated. Constraint (12e) works the same way for down-regulation. Constraint (12f) bounds the power to be between the minimum and nominal power. Constraint (12g) bounds the slack variable which is the energy not delivered as promised. Constraint (12h) is the bilinear constraint from (8). Constraint (12i) ensures that down-regulation is equal to at least 10% of the down-regulation capacity. Lastly, constraint (12j) prohibits any up-regulation when defrosting occurs.

3) Physical constraints: The state-space model in (2) is simply added as constraints with $p_{t,\omega}$ being the power of the freezer and an additional index for each scenario, ω.

Note, the freezer specific variables are indexed by t, representing a time step $dt = 0.25$ whereas all other variables are indexed by hour h.

Furthermore, there is a set of identical constraints to (2) that simulates the baseline temperatures, $T_t^{f,B}$ and $T_t^{c,B}$, using the baseline power, P_h^{Base}. These are used for the following boundary constraint, as well as the rebound constraints in Section III-E4.

$$T^f_{96,\omega} \leq T^{f,\text{Base}}_{96}, \quad \forall \omega \tag{13}$$

The boundary constraint in (13) ensures that the optimization does not exploit the end state.

Temperature constraints to the air temperature can easily be added to limit the flexibility of the TCL by introducing a maximum temperature difference to the baseline temperature, $\Delta^{\max}$:

$$T_t^{c,\text{Base}} - \Delta \leq T^c_{t,\omega}, \quad \forall t, \omega \tag{14a}$$
$$T_t^{c,\text{Base}} - \Delta \geq T^c_{t,\omega}, \quad \forall t, \omega \tag{14b}$$
$$\Delta \leq \Delta^{\max} \tag{14c}$$

4) Rebound constraints: The rebound constraints ensures that a rebound happens right after an up-regulation by down-regulating:

$$y^{\downarrow}_{h,\omega} \geq z^{\uparrow}_{h,\omega}, \quad \forall h, \omega \tag{15a}$$
$$y^{\downarrow}_{h,\omega} \leq z^{\uparrow}_{h,\omega}, \quad \forall h, \omega \tag{15b}$$

Furthermore, the following rebound constraints ensures that the rebound will take place until the food temperature is equal to the baseline food temperature, which can be considered the setpoint food temperature:

$$\sum_{t=4\cdot(h-1)}^{4h} T^{f}_{t,\omega} - T^{f,\text{Base}}_{t} \geq -(1 - z^{\downarrow}_{h,\omega}) \cdot M, \quad \forall \omega, \forall h \tag{16a}$$
$$\sum_{t=4\cdot(h-1)}^{4h} T^{f}_{t,\omega} - T^{f,\text{Base}}_{t} \leq -(1 - z^{\downarrow}_{h,\omega}) \cdot M, \quad \forall \omega, \forall h \tag{16b}$$

In constraints (16), M is a sufficiently big number such that the food temperature is allowed to deviate from the baseline.

Lastly, the following constraint ensures that up-regulation happens before down-regulation:

$$\sum_{k=0}^{h} y^{\downarrow}_{\omega,k} \leq y^{\uparrow}_{\omega,k}, \quad \forall h, \omega \tag{17}$$

This makes sense since it is not possible (or at least difficult) to anticipate potential up-regulation events in the power grid. As such, it does not make sense to pre-cool (or pre-heat) a TCL in the context of mFRR.

IV. Results and Discussion

In this section, we present and discuss the results related to providing mFRR versus load shifting for a single supermarket freezer using the optimization model in (6), and the scenarios and solution strategies described in Section III-B and III-D. First, we discuss the main result: mFRR versus load shifting. Second, we discuss the effectiveness of the ADMM solution strategy.

A. Load shifting vs mFRR

Figure 6 shows the cumulative cost for mFRR versus load shifting compared to the baseline cost. For mFRR, the lookback strategy is similar to training on 2021 data. But both of them have a higher cost than load shifting for most of the year. Interestingly, mFRR was very profitable in June where reservation prices increased significantly due to an outage of a reserve power plant.

Table II breaks down the cost components. For mFRR, there is big difference between the lookback strategy and mFRR trained on 2021 data. The lookback strategy earns much more from activation payments, but is also penalized more as it is not able to deliver its reservation capacity in some days. The other mFRR strategy bids more conservatively and is only rarely activated. All strategies are better than the baseline costs, i.e., not utilizing flexibility, with savings of 10-14%.

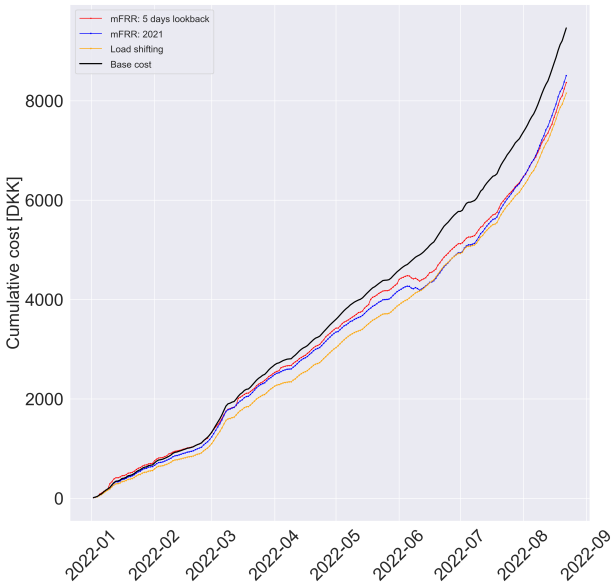

Fig. 6. OOS cumulative cost for load shifting and mFRR using ADMM with 50 scenarios trained on 2021 data (blue), and a lookback of five days (red).

TABLE II
Average Daily OOS Costs.

Name	mFRR w. lookback	Load shifting	mFRR w. 2021
Base cost today	40.628	40.628	40.628
Total cost	35.918	34.994	36.514
Expected energy cost	40.628	34.994	40.628
Rebound cost	0.858	N/A	0.911
Reserve payment	3.216	0.0	3.381
Act payment	8.092	0.0	2.161
Penalty cost	5.741	0.0	0.516
Scenarios	-5	1	50
Admm	False	False	True
% savings	11.6	13.9	10.1

In Figure 7, load shifting and mFRR are compared for the same day. For load shifting, it can clearly be seen how load is shifted to low-price hours, especially at the end of the day. But it also has a very significant effect on the temperature with large deviations from its normal setpoint. For mFRR, the reservation is almost full for all hours during the day. The activation of reservation occurs when the bid price is lower than the balancing price which in this particular scenario only happens for three hours. The effect on the temperature is therefore much smaller than for load shifting. The model is also able to rebound smartly in hour 19 to avoid high rebound costs.

The results show some interesting features of mFRR and load shifting. For load shifting, although the savings are higher, they are directly proportional to the energy shifted and therefore the temperature deviation in the freezer. For mFRR, this is not the case due to the mechanism of reservation and

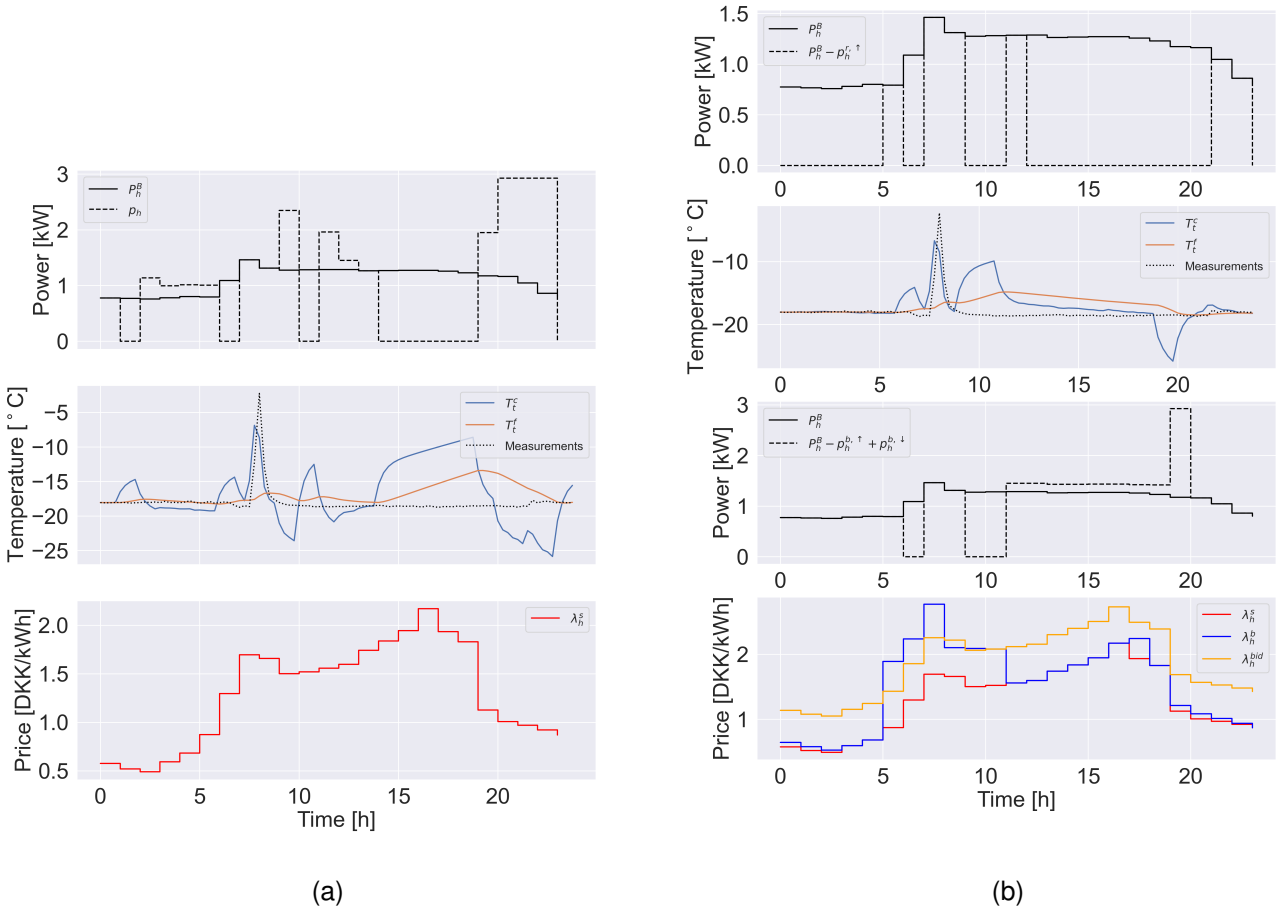

Fig. 7. Comparison between load shifting and mFRR in one IS scenario. **a**: **Top**: Power profile when load shifting and baseline power of freezer. **Middle**: Air and food temperature dynamics. **Bottom**: Spot price in scenario. **b**: **Top**: Reservation capacities and baseline power of freezer. **Upper middle**: Air and food temperature dynamics. **Lower Middle**: mFRR activations in this scenarios, i.e., when $\lambda_h^{bid} \leq \lambda_h^b$, $\lambda_h^b > \lambda_h^s$ and $p_h^{r,\uparrow} > 0$. **Bottom**: Spot price, balancing price, and bid price in scenario.

activation.

Furthermore, settlement costs of the BRP for load shifting were ignored as this reflects the reality of selfish, flexible consumers acting in their own interest. In reality, the BRP would have to pay for the settlement costs or at least buy/sell energy in the intraday market after the day-ahead market clearing and load shifting schedule. But consumers are not necessarily aware of the balance settlement and the electricity market mechanisms. Hence, they have a strong incentive to use their flexibility for load shifting. Some industrial and commercial consumers might not be exposed fully to the spot price, and for those consumers, load shifting is less profitable, but they will still have an incentive to change their deal with the retailer to get full exposure.

For mFRR, it was implicitly assumed that all revenue from reservation and payments go to the flexible consumer. But this neglect the fact that the BRP requires a share of the revenue. Furthermore, there might be an aggregator or technology provider facilitating the aggregation and communication of the flexibility. In this case, the they would also want a share of the revenue. This can potentially reduce the revenue of the consumer significantly and is one of the main challenges of achieving widespread penetration of demand-side flexibility [1].

For these reasons, load shifting seems more appealing for a flexible consumer compared to mFRR from a monetary point of view. This finding illustrates the importance of designing attractive markets for mFRR if demand-side flexibility is to be used more widely, and perhaps also to disincentivize load shifting flexible consumers as it could lead to system imbalances.

B. ADMM

Figure 8 shows the ADMM convergence to the optimal solution for five scenarios for different step sizes. For most step sizes, it converges quickly but never quite reaches the optimal solution. This is mainly because the algorithm has to achieve consensus on three variables, $p_{h,\omega}^{r,\uparrow}$, α_ω, and β_ω. Experiments showed that it was much closer to the optimal solution when removing α_ω, and β_ω.

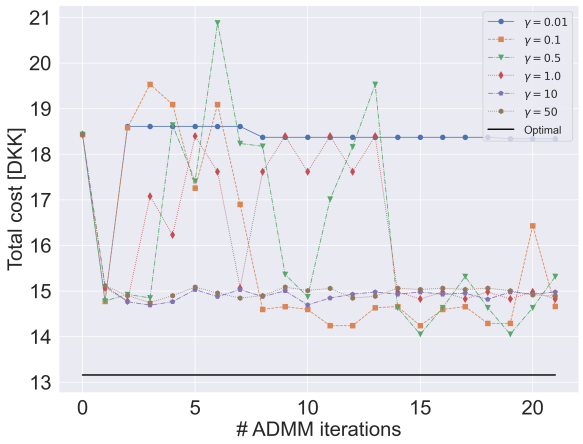

Fig. 8. ADMM solution versus the optimal solution for five scenarios for different step sizes in the ADMM algorithm.

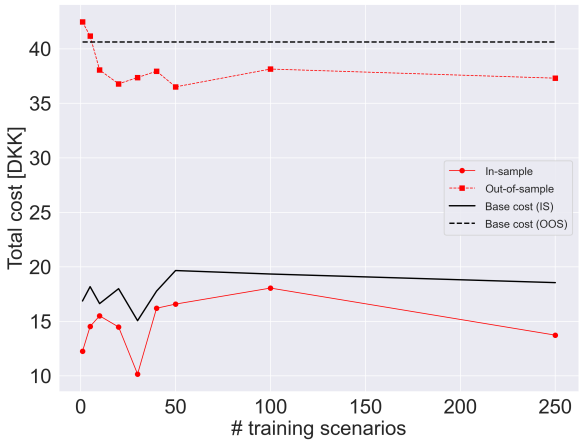

Fig. 9. Effect of number of IS scenarios on OOS performance for ADMM. Both are compared to the baseline costs of the freezer.

A large step size emphasizes the need to reach consensus whereas a small step size prioritizes the normal objective function in (6a). Here, it seems a step size of $\gamma \geq 10$ is more stable and converges quickly.

Figure 9 shows the effect of including more scenarios in Problem (6) using ADMM to solve it for both IS training and OOS evaluation. For IS training, good solution are already obtained with 10 scenarios, and the same applies for OOS although it seems using 250 scenarios also performs well.

The plot highlights the importance of choosing representative scenarios, especially balancing prices as they determine how much activation is needed, and therefore the bid policy.

V. Conclusion

In this paper, it has been investigated how a supermarket freezer can provide flexibility for mFRR and load shifting in Denmark to see which one provide the greater incentive for a flexible load. This was done by creating a second-order grey-box model of the temperature dynamics in the freezer with the food temperature as a latent state. In state-space form, the model was directly integrated as constraints in a two-stage stochastic MILP which maximizes value from flexibility from mFRR. Two solution strategies was implemented: 1) one with a five day lookback and 2) one where the policy was learned on 2021 using up to 250 scenarios and solved using ADMM decomposition. The optimization model simplified to a simple MILP for load shifting and could be solved directly. Evaluation was done on unseen 2022 price data. Load shifting was more profitable, but had a greater impact on the temperatures in the freezer as opposed to mFRR that depends on the system state and bid price for activations. However, the BRP and aggregator share of the revenue was not considered. Hence, we find that load shifting is more appealing for a flexible load which is not necessarily beneficial for the TSO and the power grid.

Acknowledgement

The authors would like to acknowledge the financial support from Innovation Fund Denmark under grant number 0153-00205B for partially funding the work in this paper. The authors would also like to thank Haris Ziras (DTU) for his feedback on the paper and his valuable input on the development of the grey-box model of the freezer. The authors would also like to thank Coop and AK-Centralen for providing the freezer and power data from a supermarket used in this paper.

References

[1] P. A. Gade, T. Skjøtskift, H. W. Bindner, and J. Kazempour, "Ecosystem for demand-side flexibility revisited: The danish solution," *The Electricity Journal*, vol. 35, no. 9, p. 107206, 2022.

[2] S. E. Shafiei, H. Rasmussen, and J. Stoustrup, "Modeling supermarket refrigeration systems for demand-side management," *Energies*, vol. 6, no. 2, pp. 900–920, 2013.

[3] L. N. Petersen, H. Madsen, and C. Heerup, "Eso2 optimization of supermarket refrigeration systems," *Technical University of Denmark, Department of Informatics and Mathematical Modeling, Tech. Rep*, 2012.

[4] R. Pedersen, J. Schwensen, S. Sivabalan, C. Corazzol, S. E. Shafiei, K. Vinther, and J. Stoustrup, "Direct control implementation of a refrigeration system in smart grid," pp. 3954–3959, 2013.

[5] R. Pedersen, J. Schwensen, B. Biegel, T. Green, and J. Stoustrup, "Improving demand response potential of a supermarket refrigeration system: A food temperature estimation approach," *IEEE Transactions on Control Systems Technology*, 2016.

[6] H. Hao, B. M. Sanandaji, K. Poolla, and T. L. Vincent, "Aggregate flexibility of thermostatically controlled loads," *IEEE Transactions on Power Systems*, vol. 30, no. 1, pp. 189–198, 2014.

[7] M. K. Petersen, K. Edlund, L. H. Hansen, J. Bendtsen, and J. Stoustrup, "A taxonomy for modeling flexibility and a computationally efficient algorithm for dispatch in smart grids," pp. 1150–1156, 2013.

[8] F. Sossan, V. Lakshmanan, G. T. Costanzo, M. Marinelli, P. J. Douglass, and H. Bindner, "Grey-box modelling of a household refrigeration unit using time series data in application to demand side management," *Sustainable Energy, Grids and Networks*, 2016.

[9] N. O'Connell, H. Madsen, P. Pinson, and M. O'Malley, "Modelling and assessment of the capabilities of a supermarket refrigeration system for the provision of regulating power," *Kgs. Lyngby*, 2013.

[10] G. De Zotti, "Leveraging consumers' flexibility for the provision of ancillary services," 2019.

[11] J. R. Schaperow, S. Gabriel, M. Siemann, and J. Crawford, "A simulation-based model for optimal demand response load shifting: a case study for the texas power market," *Journal of Energy Markets, Forthcoming*, 2019.

[12] P. Chanpiwat, S. A. Gabriel, R. L. Moglen, and M. J. Siemann, "Using cluster analysis and dynamic programming for demand response applied to electricity load in residential homes," *ASME Journal of Engineering for Sustainable Buildings and Cities*, vol. 1, no. 1, 2020.

[13] R. L. Moglen, P. Chanpiwat, S. A. Gabriel, and A. Blohm, "Optimal thermostatically-controlled residential demand response for retail electric providers," *Energy Systems*, pp. 1–21, 2020.
[14] M. Siemann, *Performance and applications of residential building energy grey-box models*. University of Maryland, College Park, 2013.
[15] I. I. Gihman and A. V. Skorohod, *The theory of stochastic processes II*. Springer, Cham, 1975.
[16] L. Bobo, S. Delikaraoglou, N. Vespermann, J. Kazempour, and P. Pinson, "Offering strategy of a flexibility aggregator in a balancing market using asymmetric block offers," 2018.
[17] Ecogrid, "Ecogrid 2.0," accessed 2022-09-30. [Online]. Available: http://ecogrid.dk/
[18] B. Biegel, P. Andersen, J. Stoustrup, L. H. Hansen, and D. V. Tackie, "Information modeling for direct control of distributed energy resources," in *American Control Conference*, 2013, pp. 3498–3504.
[19] S. Harbo and B. Biegel, "Contracting flexibility services," 2013, pp. 1–5.
[20] B. Biegel, P. Andersen, T. S. Pedersen, K. M. Nielsen, J. Stoustrup, and L. H. Hansen, "Electricity market optimization of heat pump portfolio," in *2013 IEEE International Conference on Control Applications (CCA)*. IEEE, 2013, pp. 294–301.
[21] B. Biegel, P. Andersen, J. Stoustrup, M. B. Madsen, and L. H. Hansen, "Lumped thermal household model," in *IEEE PES ISGT Europe 2013*. IEEE, 2013, pp. 1–5.
[22] R. Juhl, J. K. Møller, and H. Madsen, "ctsmr-continuous time stochastic modeling in r," *arXiv preprint arXiv:1606.00242*, 2016.
[23] H. Madsen, *Time series analysis*. Chapman and Hall/CRC, 2007.
[24] S. Boyd, N. Parikh, and E. Chu, *Distributed optimization and statistical learning via the alternating direction method of multipliers*. Now Publishers Inc, 2011.
[25] M. Hong, Z.-Q. Luo, and M. Razaviyayn, "Convergence analysis of alternating direction method of multipliers for a family of nonconvex problems," *SIAM Journal on Optimization*, vol. 26, no. 1, pp. 337–364, 2016.
[26] J. M. Morales, A. J. Conejo, H. Madsen, P. Pinson, and M. Zugno, *Integrating renewables in electricity markets: operational problems*. Springer Science & Business Media, 2013, vol. 205.

Peter A.V. Gade is an Industrial PhD researcher at IBM and affiliated with the Technical University of Denmark, Kongens Lyngby, Denmark, in the Energy Markets and Analytics Section within the Power and Energy Systems division at the Wind and Energy Systems Department. His research focuses on demand-side flexibility and the revenue streams from utilization of demand-side flexibility. He holds a M.S. in Mathematical Modelling and Computing and a B.S. in Biomedical Engineering, both from the Technical University of Denmark.

Trygve Skjøtskfit is an Associate Partner at IBM Denmark, with focus on energy transformation and demand-side flexibility. His solid experience and deep knowledge within intelligent energy systems, buildings, and civil infrastructures makes him a leading figure, strategic advisor, and a first mover in the flexibility market with a strong track record to find and deliver new cutting-edge solutions. He holds an MBA in Strategy from Universitat Pompeu Fabra, and a Master of Export Engineering from Copenhagen University, College of Engineering.

Henrik W. Bindner received the MSc in Electrical Engineering from Technical University of Denmark in 1988. He is currently a senior researcher with the Department of Wind and Energy Systems, Technical University of Denmark. He is heading the *Distributed Energy Systems* Section and his research interests include control and management of smart grids, active distribution networks, and integrated energy systems.

Jalal Kazempour is an Associate Professor with the Department of Wind and Energy Systems, Technical University of Denmark, where he is heading the *Energy Markets and Analytics* Section. He received the Ph.D. degree in Electrical Engineering from the University of Castilla-La Mancha, Ciudad Real, Spain, in 2013. His research interests include intersection of multiple fields, including power and energy systems, electricity markets, optimization, game theory, and machine learning.